

# Meson fluctuations and thermodynamics of the Polyakov loop extended quark-meson model

V. Skokov,<sup>1,\*</sup> B. Stokić,<sup>1</sup> B. Friman,<sup>1</sup> and K. Redlich<sup>2,3</sup>

<sup>1</sup>*GSI Helmholtzzentrum für Schwerionenforschung, D-64291 Darmstadt, Germany*

<sup>2</sup>*Institute of Theoretical Physics, University of Wrocław, PL-50204 Wrocław, Poland*

<sup>3</sup>*Theory Division, CERN, CH-1211 Geneva 23, Switzerland*

Thermodynamics and the phase structure of the Polyakov loop-extended two flavor chiral quark-meson model (PQM) are explored. The analysis of the PQM model is based on the functional renormalization group (FRG) method. An appropriate truncation of the effective action with quarks coupled to background gluonic fields is introduced. Within this scheme, we derive the renormalization group flow equation for the scale-dependent thermodynamic potential at finite temperature and density in the presence of a symmetry breaking external field. The influence of fluctuations and of the background gluon field on the properties of net-quark number density fluctuations and their higher moments is explored. We study the dependence of the kurtosis of quark number fluctuations on the pion mass and show that, in the presence of a symmetry breaking term, the fluctuations lead to a smoothing of observables near the crossover transition.

PACS numbers:

## I. INTRODUCTION

The phase diagram of strongly interacting matter at nonzero baryon density and high temperature has been a subject of growing interest in recent years. Calculations done within the Lattice Gauge Theory (LGT) show a clear separation between the confined-hadronic and deconfined, quark-gluon plasma phase at finite temperature [1]. Quantum Chromodynamics (QCD) exhibits both dynamical chiral symmetry breaking and confinement at finite temperature and densities. However, since QCD thermodynamics at large baryon densities is still not accessible for first principle LGT calculations, many phenomenological models and effective theories have been developed.

The hadronic properties at low energy as well as the nature of the chiral phase transition at finite temperature and densities have been successfully described and explored in such effective models. Also, the physics of color deconfinement and its relation to chiral symmetry breaking has been recently studied in terms of effective chiral models [2–13]. The idea to extend the existing chiral models, such as the Nambu–Jona–Lasinio (NJL) or the chiral quark–meson model, by introducing couplings of quarks to uniform temporal background gauge fields (Polyakov loops) was an important step forward in these studies [5, 13].

It was shown that the Polyakov loop extended Nambu–Jona–Lasinio (PNJL) [7] or quark meson (PQM)[13] models reproduce essential properties of QCD thermodynamics obtained in the LGT calculations already in the mean-field approximation. However, to correctly account for the critical behavior and scaling properties near the chiral phase transitions one needs to go beyond the mean-

field approximation and include quantum fluctuations and non-perturbative dynamics. This can be accounted for by using the functional renormalization group (FRG) [14–17]. Until now this method was applied in the NJL and quark–meson model, where the FRG equation was formulated for quarks coupled to meson fields [18–24].

In this paper we propose a truncation of the PQM model which is suitable for a functional renormalization group analysis. We introduce an additional coupling of the chiral condensate to a gluonic background via Polyakov loops. In this way the Polyakov loop dynamics is represented by a corresponding background temporal gauge field. We thus use the functional renormalization group approach in order to include fluctuations of the meson fields, while the Polyakov loop is treated on a mean-field level. Consequently, our calculation lacks an FRG description of the fluctuations of the Polyakov loops. However, already in this approximation we find an important effect of the interactions of quarks with the effective gluon fields on the thermodynamics. For comparison we also present results for the chiral quark–meson model (QM) without Polyakov loops in the FRG approach in order to make the difference in the thermodynamics of the two effective models more transparent and to emphasize the role of the gluonic background field. We also compare with the PQM and QM models in mean-field approximation.

In this study we use the Taylor expansion method to describe the thermodynamics at finite chemical potential  $\mu$ . We discuss the influence of fluctuations and the background gluon field on the properties of the net-quark number density susceptibilities. Results on the properties of generalized susceptibilities of the net quark number density in the presence of mesonic fluctuations in a gluonic background are presented. We also explore ways to reduce the dependence on the ultraviolet cutoff in the FRG approach.

The paper is organized as follows: In Sec. II we in-

---

\*E-Mail: V.Skokov@gsi.de

roduce the PQM model. In Sec. III we formulate the renormalization group equation for the thermodynamic potential in the PQM model. In Sec. IV we consider the mean-field approximation. In Sec. V we discuss the critical properties and thermodynamics of the PQM model in the presence of mesonic fluctuations.

## II. THE POLYAKOV-QUARK-MESON MODEL

The chiral quark–meson model is used as an effective realization of the low–energy sector of the QCD. However, because the local  $SU(N_c)$  invariance of QCD is replaced by a global symmetry, one cannot describe deconfinement phenomena in this model. Recently, it was argued that, by connecting the chiral quark–meson model with the Polyakov loop potential, the confining properties of QCD can be approximately accounted for [5, 12, 13]. Consequently, the Polyakov–quark–meson (PQM) model effectively combines both the chiral and confining properties of QCD.

The Lagrangian of the PQM model reads

$$\mathcal{L} = \bar{q} [i\mathcal{D} - g(\sigma + i\gamma_5\vec{\tau}\vec{\pi})] q + \frac{1}{2}(\partial_\mu\sigma)^2 + \frac{1}{2}(\partial_\mu\vec{\pi})^2 - U(\sigma, \vec{\pi}) - \mathcal{U}(\ell, \ell^*). \quad (1)$$

The coupling between the effective gluon field and the quarks is implemented through the covariant derivative

$$D_\mu = \partial_\mu - iA_\mu, \quad (2)$$

where  $A_\mu = g A_\mu^a \lambda^a/2$ . The spatial components of the gluon field are neglected, i.e.  $A_\mu = \delta_{\mu 0} A_0$ . Moreover,  $\mathcal{U}(\ell, \ell^*)$  is the effective potential for the gluon field expressed in terms of the thermal expectation values of the color trace of the Polyakov loop and its conjugate

$$\ell = \frac{1}{N_c} \langle \text{Tr}_c L(\vec{x}) \rangle, \quad \ell^* = \frac{1}{N_c} \langle \text{Tr}_c L^\dagger(\vec{x}) \rangle, \quad (3)$$

with

$$L(\vec{x}) = \mathcal{P} \exp \left[ i \int_0^\beta d\tau A_4(\vec{x}, \tau) \right], \quad (4)$$

where  $\mathcal{P}$  stands for path ordering,  $\beta = 1/T$  and  $A_4 = iA_0$ .

The  $O(4)$  representation of the meson fields is  $\phi = (\sigma, \vec{\pi})$  and the corresponding  $SU(2)_L \otimes SU(2)_R$  chiral representation is given by  $\sigma + i\vec{\tau} \cdot \vec{\pi}\gamma_5$ . There are  $N_f^2 = 4$  mesonic degrees of freedom coupled to  $N_f = 2$  flavors of quarks.

The purely mesonic potential of the model,  $U(\sigma, \vec{\pi})$ , is defined as

$$U(\sigma, \vec{\pi}) = \frac{\lambda}{4} (\sigma^2 + \vec{\pi}^2 - v^2)^2 - c\sigma, \quad (5)$$

while the effective potential of the gluon field is parametrized to preserve the  $Z(3)$  invariance:

$$\frac{\mathcal{U}(\ell, \ell^*)}{T^4} = -\frac{b_2(T)}{2} \ell^* \ell - \frac{b_3}{6} (\ell^3 + \ell^{*3}) + \frac{b_4}{4} (\ell^* \ell)^2. \quad (6)$$

The parameters,

$$b_2(T) = a_0 + a_1 \left( \frac{T_0}{T} \right) + a_2 \left( \frac{T_0}{T} \right)^2 + a_3 \left( \frac{T_0}{T} \right)^3 \quad (7)$$

with  $a_0 = 6.75$ ,  $a_1 = -1.95$ ,  $a_2 = 2.625$ ,  $a_3 = -7.44$ ,  $b_3 = 0.75$  and  $b_4 = 7.5$  were chosen to reproduce the equation of state of pure gauge degrees of freedom calculated on the lattice. At the temperature  $T_0 = 270$  MeV, the critical temperature obtained for pure gauge theory, the potential (6) yields a first order phase transition.

## III. THE FRG METHOD IN THE PQM MODEL

The functional renormalization group is an important tool for addressing nonperturbative problems within the quantum field theory. It is based on an infrared (IR) regularization with the momentum scale parameter,  $k$ , of the full propagator which turns the corresponding effective action into a scale dependent functional  $\Gamma_k$  [14–17]. The change of  $\Gamma_k$  with the change of the momentum scale is described through the flow equation:

$$\partial_k \Gamma_k[\Phi, \psi] = \frac{1}{2} \text{Tr} \left\{ \partial_k R_{kB} \left( \Gamma_k^{(2,0)}[\Phi, \psi] + R_{kB} \right)^{-1} \right\} - \text{Tr} \left\{ \partial_k R_{kF} \left( \Gamma_k^{(0,2)}[\Phi, \psi] + R_{kF} \right)^{-1} \right\}, \quad (8)$$

where  $\Gamma_k^{(2,0)}$  and  $\Gamma_k^{(0,2)}$  denote the second functional derivative of  $\Gamma_k[\Phi, \psi]$  with respect to the bosonic ( $\Phi$ ) and fermionic ( $\psi$ ) fields, respectively. These derivatives correspond to the inverse of the full propagators at the scale  $k$ . The trace in Eq. (8) denotes a momentum integration and a summation over all internal indices (e.g. flavor, color, and/or Dirac). Here  $\Phi$  and  $\psi$  denote bosonic and fermionic fields, respectively. The effective average action,  $\Gamma_k$ , governs the dynamics of a theory at a momentum scale  $k$  and interpolates between the bare action,  $\Gamma_{k=\Lambda} \equiv S$ , and the full quantum effective action,  $\Gamma_{k=0} = \Gamma$ . The regulator function,  $R_k$ , describes how the small momentum modes are cut off and is to some extent arbitrary [17]. The derivative of this function,  $\partial_k R_k$ , implements the Wilsonian idea of successively integrating out momentum shells.

In the PQM model the formulation of the FRG flow equation (8) would required an implementation of the Polyakov loop as a dynamical field. However, in this exploratory calculation we treat the Polyakov loop on the mean-field level. This allows us to formulate the FRG flow equation for the truncated effective PQM action in

Euclidean space-time ( $t \rightarrow -i\tau$ ):

$$\Gamma_k = \int d^4x \left\{ \frac{1}{2} (\partial_\mu \phi)^2 + \bar{q} \not{\partial} q + g \bar{q} (\sigma + i \vec{\tau} \cdot \vec{\pi} \gamma_5) q + U_k(\rho) \right\}, \quad (9)$$

where the field  $\rho$  is given by

$$\rho = \frac{1}{2} \phi^2 = \frac{1}{2} (\sigma^2 + \vec{\pi}^2). \quad (10)$$

The finite quark chemical potential,  $\mu$ , and the gauge

potential,  $A_0$ , are introduced through the following substitution of the time derivative

$$\partial_\tau \rightarrow \partial_\tau - (\mu + iA_4). \quad (11)$$

Since the gauge potential,  $A_0$ , is treated as an effective background gluonic field, which does not flow with the scale parameter  $k$ , the explicit contribution of the Polyakov loop potential to the truncated effective action is suppressed at this stage. Later on we will restore the Polyakov loop potential.

---

As in the previous studies [25], we employ the optimized regulator functions [26] in the numerical implementation. For bosons, this cutoff function depends only on the spatial components of the momentum,

$$R_{B,k}^{\text{opt}}(\mathbf{q}^2) = (k^2 - \mathbf{q}^2) \theta(k^2 - \mathbf{q}^2), \quad (12)$$

whereas for fermions we use [25]

$$R_{F,k}^{\text{opt}}(\mathbf{q}) = \left( \sqrt{\frac{(q_0 + i\alpha_0)^2 + k^2}{(q_0 + i\alpha_0)^2 + \mathbf{q}^2}} - 1 \right) (\not{q} + i\gamma^0 \alpha_0) \theta(k^2 - \mathbf{q}^2), \quad (13)$$

where  $\alpha_0 = \mu + iA_0$  is modified due to the coupling to the background gluon field.

Using Eq. (9), with the cutoff functions given above, and the relation  $\Omega = T \Gamma$  [27], we obtain the flow equation for the scale dependent grand canonical potential for the quark and mesonic subsystems

$$\begin{aligned} \partial_k \Omega_k(\ell, \ell^*; T, \mu) = & \frac{k^4}{12\pi^2} \left\{ \frac{3}{E_\pi} \left[ 1 + 2n_B(E_\pi; T) \right] + \frac{1}{E_\sigma} \left[ 1 + 2n_B(E_\sigma; T) \right] \right. \\ & \left. - \frac{4N_c N_f}{E_q} \left[ 1 - N(\ell, \ell^*; T, \mu) - \bar{N}(\ell, \ell^*; T, \mu) \right] \right\}. \end{aligned} \quad (14)$$

Here  $n_B(E_{\pi,\sigma}; T)$  is the bosonic distribution function

$$n_B(E_{\pi,\sigma}; T) = \frac{1}{\exp(E_{\pi,\sigma}/T) - 1}$$

with the pion and sigma energy

$$E_\pi = \sqrt{k^2 + \bar{\Omega}'_k}, \quad E_\sigma = \sqrt{k^2 + \bar{\Omega}'_k + 2\rho \bar{\Omega}''_k}.$$

where the primes denote derivatives with respect to  $\rho$  and  $\bar{\Omega} = \Omega + c\sigma$ . The functions  $N(\ell, \ell^*; T, \mu)$  and  $\bar{N}(\ell, \ell^*; T, \mu)$ , defined by

$$N(\ell, \ell^*; T, \mu) = \frac{1 + 2\ell^* \exp[\beta(E_q - \mu)] + \ell \exp[2\beta(E_q - \mu)]}{1 + 3\ell \exp[2\beta(E_q - \mu)] + 3\ell^* \exp[\beta(E_q - \mu)] + \exp[3\beta(E_q - \mu)]}, \quad (15)$$

$$\bar{N}(\ell, \ell^*; T, \mu) = N(\ell^*, \ell; T, -\mu), \quad (16)$$

are fermionic distributions, modified due to the coupling to gluons, and

$$E_q = \sqrt{k^2 + 2g^2\rho} \quad (17)$$

is the quark energy. In the absence of the background gluon field, e.g. in the QM model,  $\ell, \ell^* \rightarrow 1$  and the usual Fermi-Dirac distribution function is recovered;  $N(1, 1; T, \mu) = n_F(E_q; T, \mu) = 1/\{\exp[(E_q - \mu)/T] + 1\}$ .

In order to solve the flow equation (14), we expand  $\bar{\Omega}_k(T, \mu)$ , in a Taylor series around the scale-dependent

minimum at  $\sigma_k = \sqrt{2\rho_k}$ :

$$\overline{\Omega}_k = \sum_{i=0}^m \frac{a_{i,k}}{i!} (\rho - \rho_k)^i. \quad (18)$$

As in Ref. [25], we truncate the expansion at  $m = 3$ . The Taylor coefficients,  $a_{i,k}$ , are functions of the scale,  $k$ , the temperature,  $T$ , the chemical potential,  $\mu$ , and the Polyakov loop,  $\ell$  and  $\ell^*$ .

The minimum of the thermodynamic potential is determined by the stationarity condition

$$\left. \frac{d\Omega_k}{d\sigma} \right|_{\sigma=\sigma_k} = \left. \frac{d\overline{\Omega}_k}{d\sigma} \right|_{\sigma=\sigma_k} - c = 0. \quad (19)$$

The set of flow equations for each expansion coefficient,  $a_{i,k}$ , arising from the Eq. (18) is solved numerically with an initial cutoff  $\Lambda = 1.2$  GeV. The initial conditions,  $a_{i,k=\Lambda}$  and  $c$ , are chosen to reproduce the physical pion mass  $m_\pi = 138$  MeV, the pion decay constant  $f_\pi = 93$  MeV, the sigma mass  $m_\sigma = 700$  MeV and the constituent quark mass  $m_q = 335$  MeV at the scale  $k = 0$  in vacuum. The symmetry breaking term,  $c = m_\pi^2 f_\pi$ , corresponds to an external field and consequently does not flow. In this work, we neglect the flow of the Yukawa coupling,  $g$ .

By solving equation (18) we obtain a thermodynamic potential for the quark and mesonic subsystems,  $\Omega_{k \rightarrow 0}(\ell, \ell^*; T, \mu)$ , as a function of Polyakov loop variables  $\ell$  and  $\ell^*$ . So far these variables are arbitrary. The full thermodynamic potential in the PQM model, including quark, meson and gluon degrees of freedom is obtained by adding to  $\Omega_{k \rightarrow 0}(\ell, \ell^*; T, \mu)$  the effective gluon potential  $\mathcal{U}(\ell, \ell^*)$  from Eq. (6),

$$\Omega(\ell, \ell^*; T, \mu) = \Omega_{k \rightarrow 0}(\ell, \ell^*; T, \mu) + \mathcal{U}(\ell, \ell^*). \quad (20)$$

At a given  $T$  and  $\mu$ , the Polyakov loop variables,  $\ell$  and  $\ell^*$  are determined by the stationarity conditions:

$$\frac{\partial}{\partial \ell} \Omega(\ell, \ell^*; T, \mu) = 0, \quad (21)$$

$$\frac{\partial}{\partial \ell^*} \Omega(\ell, \ell^*; T, \mu) = 0. \quad (22)$$

---

A detailed derivation of the mean-field approximation of PMQ model can be found in Ref. [30] and references therein. Here we present only the final result for thermodynamic potential

$$\Omega_{MF} = \mathcal{U}(\ell, \ell^*) + U(\langle \sigma \rangle, \langle \pi \rangle = 0) + \Omega_{q\bar{q}}(\langle \sigma \rangle, \ell, \ell^*). \quad (23)$$

The contribution of quarks with mass  $m_q = g\langle \sigma \rangle$  is given by

$$\Omega_{q\bar{q}}(\langle \sigma \rangle, \ell, \ell^*) = -2N_f T \int \frac{d^3p}{(2\pi)^3} \left\{ \frac{N_c E_q}{T} \theta(\Lambda_{MF}^2 - p^2) + \ln g^{(+)}(\langle \sigma \rangle, \ell, \ell^*; T, \mu) + \ln g^{(-)}(\langle \sigma \rangle, \ell, \ell^*; T, \mu) \right\}, \quad (24)$$

where

$$g^{(+)}(\langle \sigma \rangle, \ell, \ell^*; T, \mu) = 1 + 3\ell \exp[-(E_q - \mu)/T] + 3\ell^* \exp[-2(E_q - \mu)/T] + \exp[-3(E_q - \mu)/T], \quad (25)$$

$$g^{(-)}(\langle \sigma \rangle, \ell, \ell^*; T, \mu) = g^{(+)}(\langle \sigma \rangle, \ell^*, \ell; T, -\mu); \quad (26)$$

Within the FRG approach, the thermodynamic potential of the QM model is obtained from Eq. (20), by dropping the effective Polyakov loop potential and setting  $\ell = \ell^* = 1$ .

In the following we explore the thermodynamics of the PQM-FRG model. The role of the gluonic sector is assessed by juxtaposing the results obtained within the PQM and QM models, while the effect of mesonic fluctuations in the PQM model are deduced by comparing with the mean-field approximation.

#### IV. THE MEAN-FIELD APPROXIMATION

The importance of mesonic fluctuations is best illustrated by comparing the FRG approach with the mean-field (MF) approximation for mesons. In the latter, both quantum and thermal fluctuations are neglected and the mesonic fields are replaced by their classical expectation values. In the formulation presented in the previous section, the mean-field approximation is recovered by omitting the pion- and sigma-meson contributions in Eq. (14). Alternatively, this approximation can be obtained directly from the partition function for the Lagrangian (1) by integrating out the quark degrees of freedom. These approaches are equivalent up to a surface term, which is negligible for large cutoffs,  $\Lambda \rightarrow \infty$ . We explicitly retain the divergent vacuum contribution, which is regularized by an ultraviolet cutoff  $\Lambda_{MF}$ . The importance of this contribution was demonstrated in Refs. [28, 29].

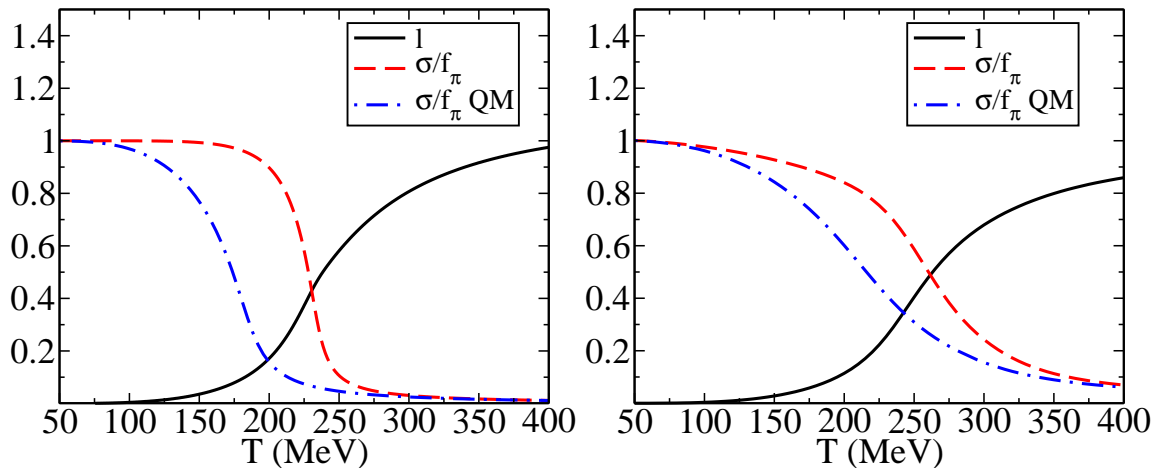


FIG. 1: Thermal average of the Polyakov loop,  $\ell$ , and of the order parameter of the chiral phase transition,  $\langle\sigma\rangle$ , as functions of temperature at zero baryon chemical potential in the mean-field approximation(left panel) and in FRG approach (right panel). The solid and dashed lines are obtained in the PQM model, while the dash-dotted lines correspond to the QM model.

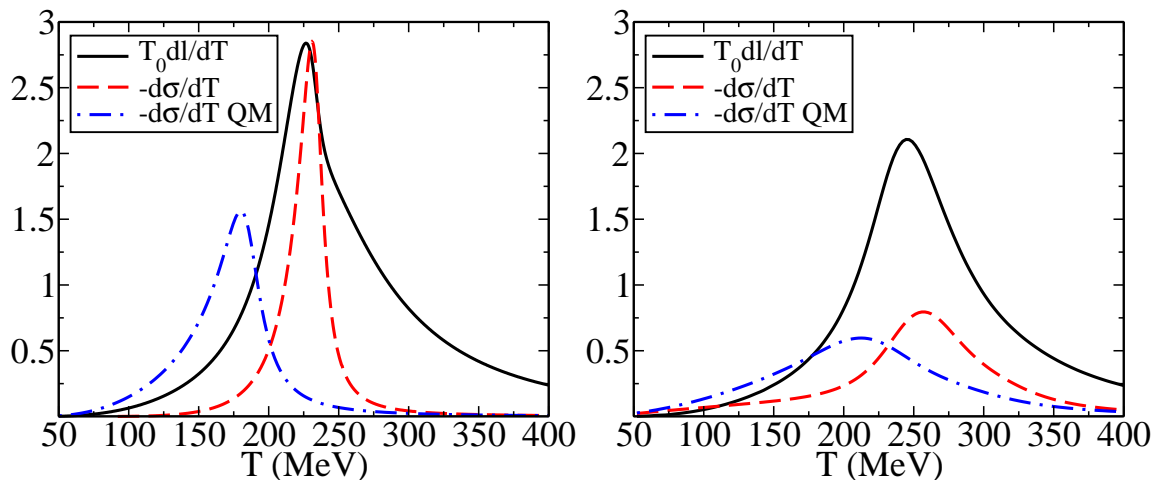


FIG. 2: Temperature derivatives of thermal average of the Polyakov loop,  $\ell$ , and of the order parameter of the chiral phase transition,  $\langle\sigma\rangle$ , as functions of temperature at zero baryon chemical potential in the mean-field approximation(left panel) and in the FRG approach (right panel). The notation is the same as in Fig. 1.

and  $E_q = \sqrt{p^2 + m_q^2}$  is the quark quasi-particle energy.

The equations of motion for the mean fields are obtained by requiring that the thermodynamic potential be stationary with respect to changes of  $\sigma$ ,  $\ell$  and  $\ell^*$ :

$$\frac{\partial\Omega_{MF}}{\partial\sigma} = \frac{\partial\Omega_{MF}}{\partial\ell} = \frac{\partial\Omega_{MF}}{\partial\ell^*} = 0. \quad (27)$$

The model parameters are fixed to reproduce the same vacuum physics as in the FRG calculation, as described in the previous section. The additional free parameter,  $\Lambda_{MF}$ , is chosen so as to reproduce the quark condensate in vacuum  $\langle\bar{u}u\rangle = -(260 \text{ MeV})^3$ ; we find  $\Lambda_{MF} = 674 \text{ MeV}$ .

## V. FLUCTUATIONS AND THERMODYNAMICS OF THE PQM MODEL

The thermodynamic potential obtained in section III can be used to explore the influence of the gluonic background field on the thermodynamics in the PQM model including the effect of fluctuations. In previous studies of the chiral quark–meson model within the FRG approach, it was shown that non-perturbative meson contributions modify the position of the chiral boundary and the critical end point (CEP) in the  $(T, \mu)$ -plane. The pseudocritical temperature and chemical potential is usually identified by a maximum in the temperature derivative of the



order parameter or in the chiral susceptibility. In Figs. 1 and 2 we show the dependence of  $\langle\sigma\rangle$  and Polyakov loop  $\ell$  and of their temperature derivatives computed in the FRG approach as well as in the mean-field approximation for the PQM and QM models.

As expected, for a physical pion mass the model exhibits a smooth crossover as a function of temperature. Moreover, as shown in Fig. 2, the temperature derivatives of both the Polyakov loop and the chiral order parameter exhibit peak structures at approximately the same temperature,  $T_c = 257$  MeV in the PQM-FRG and  $T_c = 230$  MeV in the PQM-MF model. In general the relation between the deconfinement and chiral phase transitions is not well established. Recent LGT calculations lead to conflicting conclusions concerning the relative position of these transitions [1, 31].

A comparison of the QM and PQM models shows that the inclusion of gluon degrees of freedom shifts the chiral phase transition to higher temperatures both with and without mesonic fluctuations. The latter lead to a smoothing of the transition, as shown in Figs. 1 and 2.

### A. Quark number fluctuations

To explore the influence of non-zero baryon chemical potential on the thermodynamics we employ the Taylor-expansion in  $\mu/T$  around  $\mu = 0$  applied in LGT [1] and in model calculations [32, 33]. In particular, we obtain the expansion of the thermodynamic pressure

$$\frac{p(T, \mu)}{T^4} = \sum_{n=0}^{\infty} \frac{1}{n!} c_n(T) \left(\frac{\mu}{T}\right)^n, \quad (28)$$

where

$$c_n(T) = \left. \frac{\partial^n [p(T, \mu)/T^4]}{\partial (\mu/T)^n} \right|_{\mu=0}. \quad (29)$$

The expansion coefficients  $c_n(T)$  are generalized susceptibilities that characterize the fluctuations of the net quark number  $\delta N_q = N_q - \langle N_q \rangle$  at vanishing chemical potential [34–36]. In particular, the first two non-vanishing derivatives,  $c_2$  and  $c_4$ , are the second and fourth order cumulants:

$$\begin{aligned} c_2 &= \frac{\chi_q}{T^2} = \langle (\delta N_q)^2 \rangle, \\ c_4 &= \langle (\delta N_q)^4 \rangle - 3 \langle (\delta N_q)^2 \rangle^2; \end{aligned} \quad (30)$$

where  $\chi_q$  is the regular quark number susceptibility.

The temperature dependence of the coefficients  $c_2$  and  $c_4$ , obtained in the mean-field approximation and in the FRG approach, is shown in Figs. 3 and 4. The coefficient  $c_2$  increases monotonously with temperature. In the mean-field approximation,  $c_2$  increases rapidly in the critical region and approaches the ideal gas limit at high temperatures. The FRG results show a rather different

behavior at high temperatures. The corresponding susceptibility is strongly suppressed above the chiral transition, due to the ultraviolet cutoff. The contribution of momenta beyond the cutoff to the thermodynamics is missing. In order to obtain the correct high-temperature behavior of the susceptibilities and other observables, one may supplement the FRG with the perturbative contribution of the high-momentum states. A simple model for implementing this correction was proposed in Ref. [37], where the corresponding contribution ( $k > \Lambda$ ) to the flow is approximated by that of a non-interacting gas of quarks and gluons. The flow equation for the high momentum contribution to the QM model then reads

$$\begin{aligned} \partial_k \Omega_k^\Lambda(T, \mu) &= \frac{k^3}{12\pi^2} \left\{ 2(N_c^2 - 1) [1 + 2n_B(k; T)] \right. \\ &\quad \left. - 4N_c N_f [1 - n_F(k; T, \mu) - n_F(k; T, -\mu)] \right\}, \end{aligned} \quad (31)$$

where the dynamical quark mass is neglected, i.e. we set  $E_q = k$ . For the PQM model we generalize this procedure, by including the interaction of quarks with the Polyakov loop

$$\begin{aligned} \partial_k \Omega_k^\Lambda(T, \mu) &= -\frac{N_c N_f k^3}{3\pi^2} \\ &\quad \left[ 1 - N(\ell, \ell^*; T, \mu) - \bar{N}(\ell, \ell^*; T, \mu) \right]. \end{aligned} \quad (32)$$

Since the effective gluon potential,  $\mathcal{U}(\ell, \ell^*)$ , is fitted to reproduce the Stefan Boltzmann limit at high temperatures, the explicit gluon contribution is omitted for consistency.

We thus proceed as follows: Eq. (31) or Eq. (32) is integrated from  $k = \infty$  to  $k = \Lambda$ , where we switch to the QM or PQM flow equation, Eq. (14). The divergent terms in the high-momentum flow equations (31-32) are independent of mesonic and gluonic fields, and of temperature and chemical potential. Consequently, they can be absorbed in an unobservable constant shift of the thermodynamic potential.

In the right panels of Figs. 3 and 4 we show the results for  $c_2$  and  $c_4$  in both the QM and PQM models. We find a smooth transition between the high and low energy regimes of the theory. The Stefan Boltzmann limit,  $c_2 = 2$ , is reproduced at high temperatures.

In contrast to  $c_2$ , the coefficient  $c_4$  shows a non-monotonic behavior near the chiral pseudocritical temperature. As shown in Fig. 4,  $c_4$  exhibits a pronounced peak at the pseudocritical temperature. The shape of the peak is changed considerably when mesonic fluctuations are included; its maximum value is reduced while the width is enhanced. We note that the peak value obtained in the mean-field approximation is strongly dependent on the cutoff  $\Lambda_{MF}$ , used to regularize the divergent vacuum contribution. A smaller value of the cutoff yields a larger maximum value of  $c_4$ . The significance of the fermion vacuum contribution was recently emphasized in Refs. [28, 29].

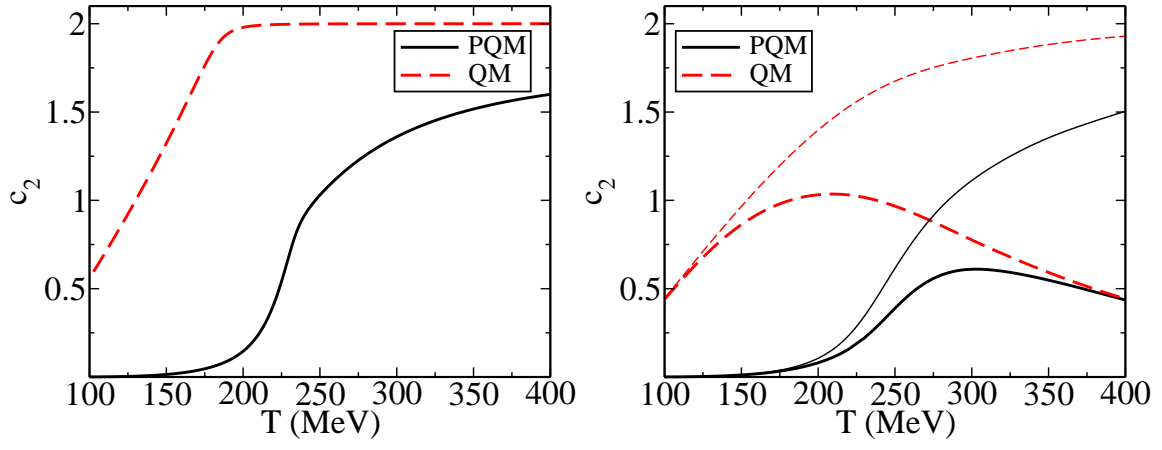


FIG. 3: The coefficient  $c_2$  as a function of temperature at zero baryon chemical potential for the PQM and QM models in the mean-field approximation (left panel) and in the FRG approach (right panel). The thin lines in the rightpanel indicate the FRG results after inclusion of the high-momentum flow (see text for details).

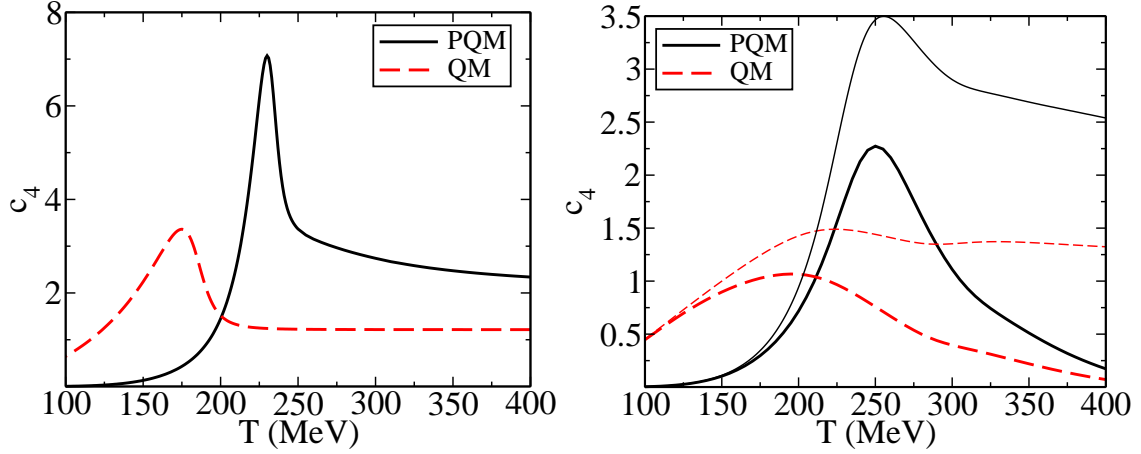


FIG. 4: The coefficient  $c_4$  as a function of temperature at zero baryon chemical potential for the PQM and QM models in the mean-field approximation (left panel) and in the FRG approach (right panel). As in Fig. 3, the thin lines indicate the FRG results after inclusion of the high-momentum flow (see text for details).

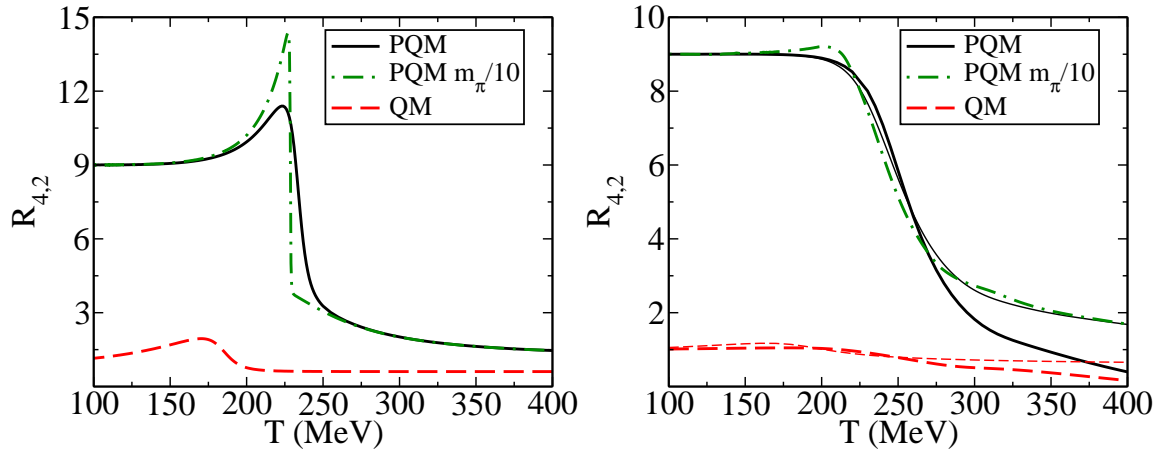


FIG. 5: The kurtosis  $R_{4,2}$  as a function of temperature at zero baryon chemical potential for the PQM and QM models in the mean-field approximation (left panel) and in the FRG approach (right panel). The thin lines indicate the FRG results after inclusion of the perturbative high-momentum modes (see text for details).

The general trends of the mean-field calculation can be inferred from Landau's theory of critical phenomena, where the thermodynamic potential is assumed to be a polynomial in the order parameter  $\sigma$

$$\Omega(T, \mu; \sigma) = \Omega_{bg}(T, \mu) + \frac{1}{2}a(T, \mu)\sigma^2 + \frac{1}{4}b\sigma^4 + c\sigma. \quad (33)$$

Here  $\Omega_{bg}(T, \mu)$  is a background contribution, independent of  $\sigma$ , and  $c$  is a symmetry breaking term. The coefficient  $a$  is generally assumed to be a linear function of the temperature,  $a = A \cdot (T - T_c)$ , where  $T_c$  is the critical temperature of the second-order phase transition for  $c = 0$ . An extension to small, non-zero values of the chemical potential is achieved by assuming

$$a(T, \mu) = A \cdot (T - T_c) + B\mu^2, \quad (34)$$

where both coefficients  $A$  and  $B$  are positive. In general the effective quartic coupling constant,  $b > 0$ , also depends on temperature and chemical potential. However this dependence is irrelevant for  $T \simeq T_c$  and  $\mu \simeq 0$ . In the chiral limit,  $c = 0$ , the  $c_2$  and  $c_4$  coefficients are easily obtained from Eq. (33):

$$c_2 = c_{2bg} + \frac{AB}{bT} \frac{T - T_c}{T} \theta(T_c - T), \quad (35)$$

$$c_4 = c_{4bg} + \frac{6B^2}{b} \theta(T_c - T). \quad (36)$$

Thus,  $c_2$  is not differentiable at the critical point, while  $c_4$  exhibits a discontinuity. The background parts,  $c_{2bg}$  and  $c_{4bg}$ , are smooth functions of temperature and do not change the critical behavior. For a finite pion mass ( $c \neq 0$ ), the transition is of the cross over type and the sharp structures in  $c_2$  and  $c_4$  are smoothened. Consequently, in the QM and PQM models, the peak structure appearing in  $c_4$  is due to the decreasing quark mass, and thus closely connected to the restoration of chiral symmetry. By contrast, in the resonance gas model, the peak in  $c_4$  is due to the increasing contribution of higher resonances.

In general, the singular part of thermodynamic potential is in chiral limit controlled by the critical exponents of the tree-dimensional O(4) symmetric spin model. Consequently, at zero chemical potential:

$$\Omega_{sing} \sim (T - T_c)^{2-\alpha}, \quad (37)$$

$$c_{2sing} \sim (T - T_c)^{1-\alpha}, \quad (38)$$

$$c_{4sing} \sim (T - T_c)^{-\alpha}. \quad (39)$$

Critical fluctuations renormalize the exponent  $\alpha$  from its mean-field value  $\alpha_{MF} = 0$  to  $\alpha = -0.21$ . Consequently, fluctuations lead to a weakening of the singularity in the chiral limit. This is reflected in a smoothening of the temperature dependence for finite pion mass, as seen in Figs. 3 and 4. We note that in QCD the singularity in  $c_2$  and  $c_4$  may be obscured by resonances, which presumably dominate the thermodynamics of the low-temperature phase.

A non-vanishing background gluon field leads to qualitative changes of the quark fluctuations. In the low-temperature phase, there is a strong suppression of the quark fluctuations due to their coupling to the Polyakov loop (see Figs. 3 and 4). This is because single and double quark modes are suppressed, when the expectation value of the Polyakov loop,  $\ell$  and  $\ell^*$ , is small (see Eqs. (14,15) and (24,25)).

Lattice studies of QCD at finite temperature and density as well as chiral model calculations show, that the ratio (kurtosis)

$$R_{4,2} = \frac{c_4}{c_2} \quad (40)$$

is an useful probe of the deconfinement and chiral phase transitions [35, 36, 38]. In the high and low temperature regimes, the kurtosis reflects the net quark content of the dominant baryon number carrying effective degrees of freedom [35, 38].

In Fig. 5 we show the ratio  $R_{4,2}$  as a function of temperature. Both in the FRG approach and in the mean-field approximation for the PQM model, the kurtosis drops from  $R_{4,2} \simeq 9$  to  $R_{4,2} < 1$  in the transition region, as expected due to the change in quark content of the baryon carrying effective degrees of freedom [35]. At low temperatures the effective three quark states dominate, while at high temperatures single quarks prevail. In the mean-field approximation (see the left panel of Fig. 5), the kurtosis exhibits a well defined peak at the transition temperature. The height of the peak depends on the value of the pion mass [38, 39]. This dependence is illustrated in Fig. 5 both in the mean-field approximation and in the FRG approach. The inclusion of mesonic fluctuations weakens the dependence on the pion mass. Thus, for a physical value of  $m_\pi$ , the kurtosis decreases monotonously with temperature in the FRG approach. A peak in  $R_{4,2}$  appears only for a pion mass below its physical value. In the mean-field approximation, the dependence on the pion mass is more pronounced, but still not as dramatic as found in Ref. [38]. This is due to the different treatments of the divergent fermion vacuum contribution. In Ref. [38] the vacuum term was subtracted at  $T = 0$  and its dependence on temperature was neglected. Here we regularize the vacuum term with an ultraviolet cut off and retain its temperature dependence, which is due to the in-medium quark mass. The role of the vacuum term in mean-field calculations and its influence on the chiral phase transition are explored in detail in Ref. [29].

In effective quark models where the Polyakov loop is neglected, the thermodynamics is governed by one-quark states at all temperatures. Consequently, in the QM model the low-temperature limit of the kurtosis is  $R_{4,2} = 1$  rather than 9. Consequently, in such models, the interaction of quarks with the background Polyakov loop is essential for reproducing the low-temperature behavior of  $R_{4,2}$  found in LGT calculations.



## VI. SUMMARY AND CONCLUSIONS

We have discussed thermodynamic properties of the Polyakov loop extended quark–meson effective chiral model (PQM), including fluctuations within the functional renormalization group method (FRG). A truncation of the PQM model was introduced, which allowed us to extend previous renormalization group studies by introducing the coupling of fermions to the Polyakov loop. We have thus formulated and solved the flow equation for the scale dependent thermodynamic potential at finite temperature and density in the presence of a background gluonic field.

In our studies of the thermodynamics we have discussed the role of fluctuations on the critical properties of the model. The fluctuations of the net quark number density and the ratio of the fourth to second order cumulants, the kurtosis, were analyzed.

Furthermore, a comparison of the FRG approach with and without a gluon background field was performed. The influence of ultraviolet cutoff effects on the thermo-

dynamics within the FRG approach was also discussed. We have shown that the FRG extended quark–meson model preserves the basic properties of the kurtosis, obtained in LGT calculations only if the Polyakov loop is included in the flow equation. Thus, the extension of the FRG method proposed here, accounting for the coupling of fermions to background gluon fields, is of particular relevance for effective descriptions of QCD thermodynamics near the phase transition in terms of the quark–meson model.

## Acknowledgment

We acknowledge fruitful discussions with E. Nakano and B.J. Schaefer. V.S. acknowledges stimulating discussions with K. Fukushima. K.R. acknowledges partial support from the Polish Ministry of Science (MEN) and the Alexander von Humboldt Foundation (AvH). B.S. gratefully acknowledges financial support from the Helmholtz Research School on Quark Matter Studies.

- 
- [1] M. Cheng et al., *Phys. Rev. D* **77**, 014511 (2008).
  - [2] A. Gocksch and M. Ogilvie, *Phys. Rev. D* **31**, 877 (1985).
  - [3] M. Buballa, *Phys. Rept.* **407**, 205 (2005).
  - [4] P. N. Meisinger and M. C. Ogilvie, *Phys. Lett. B* **379**, 163 (1996); P. N. Meisinger, T. R. Miller and M. C. Ogilvie, *Phys. Rev. D* **65**, 034009 (2002).
  - [5] K. Fukushima, *Phys. Lett. B* **591**, 277 (2004).
  - [6] F. Sannino, *Phys. Rev. D* **66**, 034013 (2002); A. Mocsy, F. Sannino and K. Tuominen, *Phys. Rev. Lett.* **92**, 182302 (2004).
  - [7] C. Ratti, M. A. Thaler and W. Weise, *Phys. Rev. D* **73**, 014019 (2006).
  - [8] C. Sasaki, B. Friman and K. Redlich, *Phys. Rev. D* **77**, 034024 (2008). *Phys. Rev. Lett.* **99**, 232301 (2007). *Phys. Rev. D* **75**, 074013 (2007).
  - [9] S. Dikal, E. Laermann and H. Satz, *Eur. Phys. J. C* **18**, 583 (2001).
  - [10] E. Megias, E. Ruiz Arriola and L. L. Salcedo, *Phys. Rev. D* **74**, 065005 (2006).
  - [11] E. M. Ilgenfritz and J. Kripfganz, *Z. Phys. C* **29**, 79 (1985).
  - [12] K. Fukushima, *Phys. Lett. B* **553**, 38 (2003); *Phys. Rev. D* **68**, 045004 (2003).
  - [13] B. J. Schaefer, J. M. Pawłowski and J. Wambach, *Phys. Rev. D* **76**, 074023 (2007).
  - [14] C. Wetterich, *Phys. Lett. B* **301**, 90 (1993).
  - [15] T. R. Morris, *Int. J. Mod. Phys. A* **9**, 2411 (1994).
  - [16] U. Ellwanger, *Z. Phys. C* **62**, 503 (1994).
  - [17] J. Berges, N. Tetradis and C. Wetterich, *Phys. Rept.* **363**, 223 (2002).
  - [18] D. U. Jungnickel and C. Wetterich, *Phys. Rev. D* **53**, 5142 (1996).
  - [19] J. Berges, D. U. Jungnickel and C. Wetterich, *Eur. Phys. J. C* **13**, 323 (2000).
  - [20] B. J. Schaefer and J. Wambach, *Nucl. Phys. A* **757**, 479 (2005).
  - [21] J. Berges, D. U. Jungnickel and C. Wetterich, *Phys. Rev. D* **59**, 034010 (1999).
  - [22] N. Tetradis, *Nucl. Phys. A* **726**, 93 (2003).
  - [23] B. J. Schaefer and H. J. Pirner, *Nucl. Phys. A* **660**, 439 (1999).
  - [24] B. J. Schaefer and J. Wambach, *Phys. Rev. D* **75**, 085015 (2007).
  - [25] B. Stokic, B. Friman and K. Redlich, arXiv:0904.0466 [hep-ph].
  - [26] D. F. Litim, *Phys. Rev. D* **64**, 105007 (2001).
  - [27] C. Wetterich, *Phys. Rev. B* **75**, 085102 (2007).
  - [28] E. Nakano, B. J. Schaefer, B. Stokic, B. Friman and K. Redlich, arXiv:0907.1344 [hep-ph].
  - [29] B. Friman, E. Nakano, K. Redlich, B. J. Schaefer and V. Skokov, work in progress.
  - [30] B. J. Schaefer, J. M. Pawłowski and J. Wambach, *Phys. Rev. D* **76** (2007) 074023 [arXiv:0704.3234 [hep-ph]].
  - [31] Y. Aoki, Z. Fodor, S. D. Katz and K. K. Szabo, *Phys. Lett. B* **643**, 46 (2006).
  - [32] C. Ratti, S. Roessner, M. A. Thaler and W. Weise, *Eur. Phys. J. C* **49**, 213 (2007).
  - [33] S. K. Ghosh, T. K. Mukherjee, M. G. Mustafa and R. Ray, *Phys. Rev. D* **73**, 114007 (2006).
  - [34] C. R. Allton, S. Ejiri, S. J. Hands, O. Kaczmarek, F. Karsch, E. Laermann and C. Schmidt, *Phys. Rev. D* **68**, 014507 (2003).
  - [35] S. Ejiri, F. Karsch and K. Redlich, *Phys. Lett. B* **633**, 275 (2006).
  - [36] F. Karsch, S. Ejiri and K. Redlich, *Nucl. Phys. A* **774**, 619 (2006); S. Ejiri, et al., *Nucl. Phys. A* **774**, 837 (2006).
  - [37] J. Braun, K. Schwenzer and H. J. Pirner, *Phys. Rev. D* **70**, 085016 (2004).
  - [38] B. Stokic, B. Friman and K. Redlich, *Phys. Lett. B* **673** (2009) 192 [arXiv:0809.3129 [hep-ph]].
  - [39] F. Karsch, PoS CPOD07,026 (2007). C. Schmidt, et. al. arXiv:0805.0236 [hep-lat]. F. Karsch, Talk given at the

- INT Conference "The QCD Critical Point" (INT-08-2b) (2008).
- [40] C. Sasaki, B. Friman and K. Redlich, Phys. Rev. D **75**, 074013 (2007).
- [41] G. Boyd, J. Engels, F. Karsch, E. Laermann, C. Legeland, M. Lutgemeier and B. Petersson, Nucl. Phys. B **469**, 419 (1996).
- [42] F. Karsch, E. Laermann and A. Peikert, Phys. Lett. B **478**, 447 (2000).